Supporting Information

Hoebeek et al. 10.1073/pnas.0907118107

SI Materials and Methods

All procedures adhered to the European guidelines for the care and use of laboratory animals (Council Directive 86/6009/EEC). Protocols were also approved by the Dutch national Animal Experiment Committee (DEC).

In Vivo Extracellular Recordings of Cerebellar Nuclei Neurons During Stimulation of the Cerebellar Cortex. A total of six adult (10–20 week old) C57BL/6 mice were prepared for chronic extracellular recordings in cerebellar nuclei (CN) as described previously (1). In short, a dental acrylic pedestal (Kemdent) was placed on the frontal, medial, and temporal bones with two 1-mm diameter stainless steel screws implanted in the frontal bone to record the EEG and one implanted in the temporal bone as reference for the recordings. During the same surgery, two 2-mm craniotomies were made in the occipital bone, which allowed entry to all CN and were covered with corticosteroid-, tetracycline-, and polymyxin-containing ointment (Pfizer) and sealed with bone wax. Following a recovery period of 5 d, extracellular recordings were obtained by advancing custom-made borosilicate glass capillaries (World Precision Instruments) filled with 0.5% NaCl and a resistance of 3 to 8 MΩ through the cerebellar cortex. CN units were identified in the interposed nuclei by the characteristic sound, location (2), and density of neurons. First, we recorded spontaneous activity for ≥60 s from each neuron. Next, the cerebellar cortex at paramedian lobules VI/VII was stimulated using custom-made bipolar-tungsten electrodes (tip distances approximately 25 μm) placed no deeper than 0.5 mm to activate the apex of the cerebellar cortex. Either a 100-Hz train of 10 pulses (80 μs), or a single 80-μs pulse of two times the strength needed to induce a pause in the action potential firing (typically 100–300 μA) was used to activate the cerebellar cortex at 0.5 Hz for 50 to 200 times. The single-unit CN neuron recordings were subsequently amplified, filtered, and digitized using a CyberAmp (Axon Instrument, Inc.) and CED1401 [Cambridge Electronic Devices (CED)], and stored for off-line analysis.

In Vivo Whole-Cell Recordings in CN Neurons During Stimulation of the Cerebellar Cortex. Thirteen adult (>10 weeks) C57BL/6 mice were prepared by placing a pedestal on the skull under isoflurane anesthesia (1.5% in 0.5 L/min O_2 and 0.2 L/min air). On the day of the experiment, animals were anesthetized with an initial i.p. injection of a saline-based ketamine/xylazine mixture (75 and 12 mg/kg, respectively) and supplemented when needed. Animals were kept at 37 °C via a custom-made feedback-controlled heating pad. After fixation of the mouse in the setup, the cerebellar cortex was revealed, the *dura mater* removed, and a stimulation electrode (tip separation ~100 μm, Micro Probe) was placed no deeper than 0.5 mm to activate lobules 6 and 7. Whole-cell recordings of CN neurons were made using borosilicate glass electrodes (Hilgenberg) with 1- to 2-μm tips and 8 to 12 MΩ, filled with internal solution (in mM: 10 KOH, 3.48 $MgCl_2$, 4 NaCl, 129 K-Gluconate, 10 hepes, 17.5 glucose 4 Na_2ATP, and 0.4 Na_3GTP), amplified with a Multiclamp 700B amplifier (Axon Instruments), and digitized with a Digidata 1440 (Axon Instruments). Stimulation intensity ranged typically from 100–300 μA, but was always approximately two times the threshold for evoking inhibitory postsynaptic potential (IPSPs). Junction potential between the electrode and the extracellular milieu was determined to be −8.53 ± 0.87 mV and corrected for in all figures. Analysis was performed using Clampfit (Axon Instruments) and custom written routines in MATLAB (Mathworks).

In Vivo Extracellular Recordings of CN Neurons During Electrical Stimulation of the Inferior Olivary Complex. Eleven adult male Wistar rats (250–300 g) were anesthetized with an i.p. injection of a ketamine/xylazine mixture (100 mg/kg and 3 mg/kg, respectively). Surgical levels of anesthesia were monitored by the absence of rhythmic whisker movements and pinch withdrawal reflexes. Supplementary doses were administered to maintain surgical levels of anesthesia. Body temperature and heart rate were constantly monitored and kept within physiological limits. Rats were mounted in a Kopf stereotactic device and the posterior cerebellum was reached by enlarging the foramen magnum (3). A small craniotomy was performed to reach the area of the red nucleus (RN) from a vertical dorsal approach with a tungsten stimulation electrode. Determination of the RN stimulation site was based on stereotactic coordinates (4) in combination with recording typical and vigorous activity of large RN units. The RN stimulation electrode served to identify cerebellar nuclear neurons by their antidromic activation in combination with collision tests and high-frequency stimulation (5). A second tungsten stimulation electrode was placed in the inferior olive (IO), which was reached at an angle of 45° with the vertical axis through the opened and enlarged foramen magnum and by entering the brainstem at approximately the anterior-posterior level of the obex. Determination of the stimulation site was based on recording the characteristic rhythm and spike appearance of IO units (3). The IO stimulation electrode served to trigger graded stimulation of climbing fibers. Recordings of units in the CN were obtained with a glass micropipette filled with 2 M NaCl and a tip of 3 to 5 μm. In two rats, a third craniotomy was made to reach the decussation of the superior cerebellar peduncle (stereotactic coordinates according to ref. 4). Using a glass pipette (tip 8–12 μm), 100 to 200 nL of lidocaine hydrochloride (2%) could be injected into the decussation. Recordings were amplified, digitized and stored on hard disk for off-line analysis (Spike 2, CED and MATLAB, Mathworks).

Data Analysis. Extracellularly recorded spikes were discriminated using Spike2 software and analyses using raster and peristimulus time plots provided by the package or by custom-made MATLAB (Mathworks) routines. Spontaneous activity patterns in the awake mice were analyzed by calculating their firing frequency and regularity of firing. To quantify the regularity of the whole recording we used the coefficient of variance [CV1 = SD (all ISIs)/mean (all ISIs)] and for the regularity of firing on small timescales we used the CV2 measure [$CV2 = 2 \mid ISI_{n+1} - ISI_n \mid / (ISI_n + ISI_{n+1})$] (see also ref. 6). To calculate significant changes in the firing frequency to the stimuli applied to the cerebellar cortex, the mean and distribution of last six ISIs before the stimulus were compared with the first three or six ISIs after the stimulus using a one-way ANOVA-test (7). To calculate significant changes in the firing frequency following olivary stimulations, the mean and distribution of ISIs during 250 ms before the stimulus was compared with the means and distributions of ISIs during 50, 100, and 250 ms after the pause using a two-sample Student's *t* test assuming nonequal variances (5). Data are represented as mean ± SEM unless indicated otherwise.

Analysis of Timed-Spiking. To quantify timed responses to stimuli presented, we analyzed spiking responses following stimulation of the cerebellar cortex by convolving the spikes with a Gaussian distribution (modified from ref. 8) to obtain the normalized Gaussian-convolved chance of spiking (Fig. S2). To do so, each

spike was replaced by a Gaussian distribution with its mean aligned to the spike time and a standard deviation of 1 ms. Then, all Gaussian distributions were aligned to the stimuli as done for a typical raster plot. Next, we normalized the summed Gaussian to the mean amplitude found during the 1-s prestimulus. We used the resulting normalized mean and SD to locate episodes of significantly increased (> +3 SD; i.e., $P < 0.001$) or decreased (<−3 SD) chance of spiking. CN neurons that displayed episodes with a significantly increased chance of spiking immediately following the stimulus induced pause were marked as showing timed-spiking rebound activity. The latency of the timed-spiking activity was calculated as the time between the end of the stimulus and the first time the mean Gaussian-convolved chance of spiking surpassed the +3 SD line. The duration of the timed-spiking activity indicates the total time that the chance of spiking was elevated during the first 100 ms poststimulus.

Stimulus-induced changes of the membrane potential were determined by obtaining the mean and SD of the subthreshold membrane potential before the stimulus. The subthreshold membrane potential was obtained by removing all spikes ± 2.5 ms from the peak. The mean resting membrane potential was calculated by averaging 130 ms before the stimulus, and deviations of >3 SD following the stimulus were considered to be significant. Because the resting membrane potential of the recorded neurons is only known from these traces, we place the words "hyperpolarization" and "depolarization" in quotation marks when used for the first time in the main text.

Spontaneous rebounds were analyzed using 1 to 3 min of continuous recordings of spontaneous activity in a similar way to the stimulus-induced rebound spiking, but instead of aligning the spikes to a stimulus, the spikes were aligned to significant spontaneous hyperpolarizations of the membrane potential. Spontaneous hyperpolarizations are obtained by smoothing the subthreshold membrane potential using a 1-s Gaussian filter. The mean and standard deviation was then determined over the whole trace and all hyperpolarizations of >3 SD from the mean were marked as spontaneous hyperpolarizations and were subsequently used to align the spikes.

Note that the use of the above described Gaussian convolution methods introduces a potential artifact when the firing frequency is low and irregular, and thus the SD is high relative to a low mean-firing frequency. In such recordings, we probably underestimated the responsiveness by setting our significant response level to 3× SD.

1. Hoebeek FE, Khosrovani S, Witter L, De Zeeuw CI (2008) Purkinje cell input to cerebellar nuclei in tottering: ultrastructure and physiology. *Cerebellum* 7:547–558.
2. Paxinos G, Franklin KBJ (2001) *The Mouse Brain in Stereotaxic Coordinates.* (Academic Press, San Diego).
3. Ruigrok TJ, Teune TM, van der Burg J, Sabel-Goedknegt H (1995) A retrograde double-labeling technique for light microscopy. A combination of axonal transport of cholera toxin B-subunit and a gold-lectin conjugate. *J Neurosci Methods* 61(1-2):127–138.
4. Paxinos G, Watson C (1998) *The Rat Brain in Stereotaxic Coordinates* (Academic Press, San Diego).
5. Ruigrok TJ (1997) Cerebellar nuclei: The olivary connection. *Prog Brain Res* 114: 167–192.
6. Wulff P, et al. (2009) Synaptic inhibition of Purkinje cells mediates consolidation of vestibulo-cerebellar motor learning. *Nat Neurosci* 12:1042–1049.
7. Alviña K, Walter JT, Kohn A, Ellis-Davies G, Khodakhah K (2008) Questioning the role of rebound firing in the cerebellum. *Nat Neurosci* 11:1256–1258.
8. Gauck V, Jaeger D (2000) The control of rate and timing of spikes in the deep cerebellar nuclei by inhibition. *J Neurosci* 20:3006–3016.

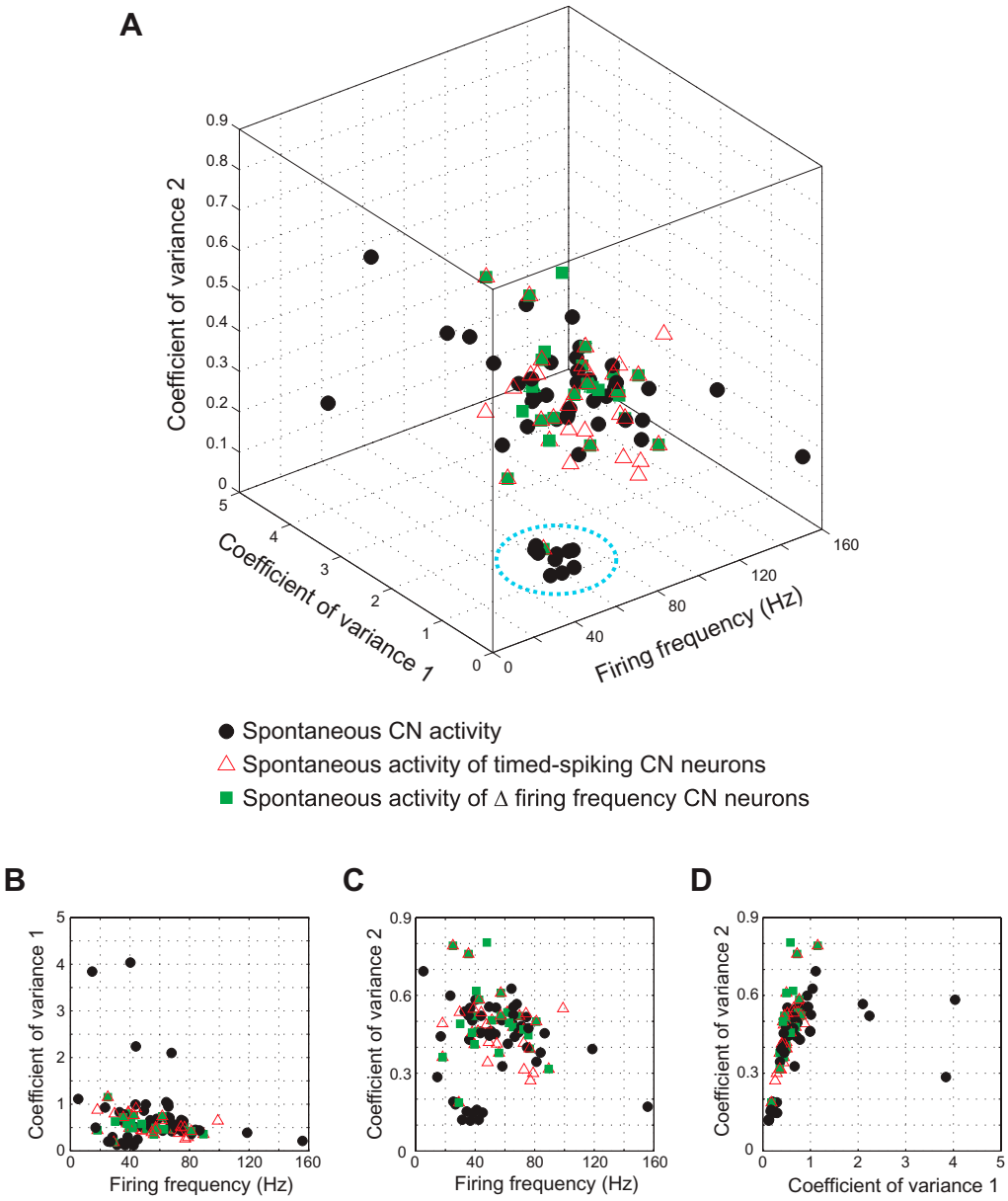

Fig. S1. (*A*) Three-dimensional plot of the baseline firing characteristics of all cerebellar nuclei (CN) neurons recorded in awake, behaving mice. Black dots indicate firing frequency vs. coefficient of variance 1 (CV1) vs. coefficient of variance 2 (CV2) of the spontaneous activity and act as a reference frame to qualify the firing characteristics of CN neurons from which we recorded. CV1 is indicative of the variation in interspike interval (ISI) length and increases with irregularity. CV2 is indicative of the temporal pattern in that it represents the mean ratio between two consecutive ISIs (*SI Materials and Methods*). As with CV1-values, CV2-values are increased in neurons that fire more irregularly. Red triangles indicate the baseline firing characteristics of CN neurons that responded to a single pulse or 10 pulses at 100 Hz stimuli with a period of timed-spiking (see main text; Fig. 1 *C*, *D*, *G*, and *H*). Green squares indicate the average baseline characteristics of neurons that responded with a significantly increased firing frequency during the first six ISIs following a single pulse or 10 pulses at 100-Hz stimulus (main text and Fig. 1 *B* and *D*). (*B*) *x-y* axis plot of 3D-plot in *A*. (*C*) *x-z* axis plot of 3D-plot in *A*. (*D*) *y-z* axis plot of 3D-plot in *A*. Overlaying triangles and squares indicate CN neurons that responded with both timed-spiking and increased firing frequency. Note the strong polarization in the represented characteristics in that 10 of the 50 neurons show very regular and slow firing patterns (blue dashed ellipse) and that apparently only one, single CN neuron that responded to electrical stimulation showed such regular and slow spiking activity.

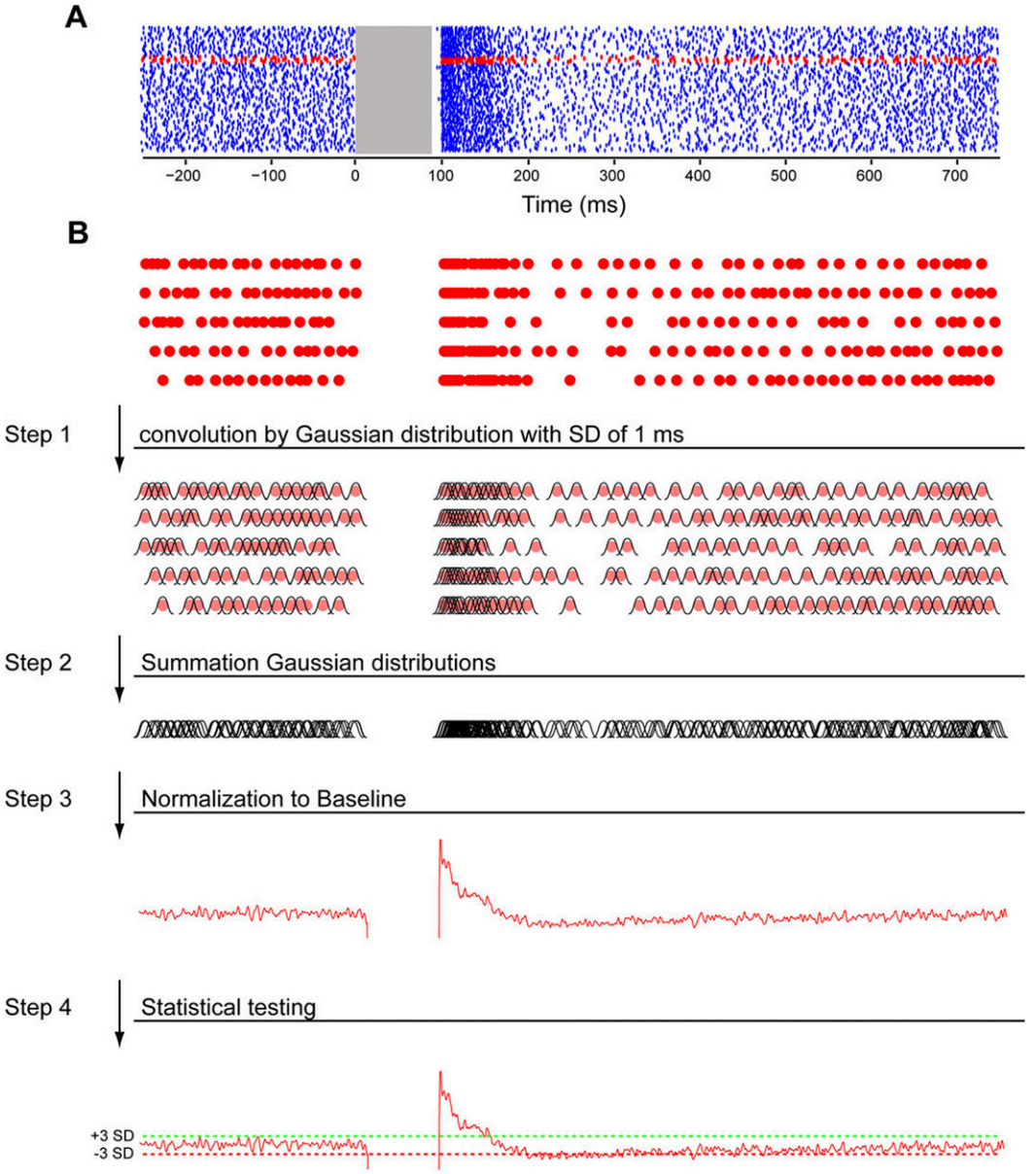

Fig. S2. (*A*) Raster plot of response of a CN neuron from the interposed nucleus to 100 repeats of an electrical (200 μA) stimulus train (10 pulses at 100 Hz) at the paravermal region of lobule VI/VII. Each dot indicates a single spike and each line a single repeat of the stimulus cycle. The gray bar indicates length of stimulus train, including 1 ms for each stimulus artifact (total of 91 ms) (*B*) (*Upper*) Enlargement of five repeats indicated in red dots in *A*. (*Lower*) To calculate timed-spiking activity (main text and Fig. 1 *C*, *D*, *G*, and *H*) we replaced each dot by a Gaussian distribution with a 1 ms SD (Step 1). Next, we summated these Gaussian distributions (Step 2), after which we normalized to the average Gaussian amplitude calculated over 1 s before the stimulus (Step 3). Finally, we calculated the SD of the baseline activity using the 1 s of activity before each stimulus, and we considered the change in episodes significant, if the amplitude was lower or higher than > 3-times SD (Step 4). If such significant episodes were found directly after a stimulus induced pause, the neuron was considered to show a timed-spiking response. The latency of such responses was calculated as the time between the end of the stimulus and the first intersection with the +3 SD line, and the duration was calculated from this latter point until the chance of spiking fell below the +3 SD line again (*SI Materials and Methods*).

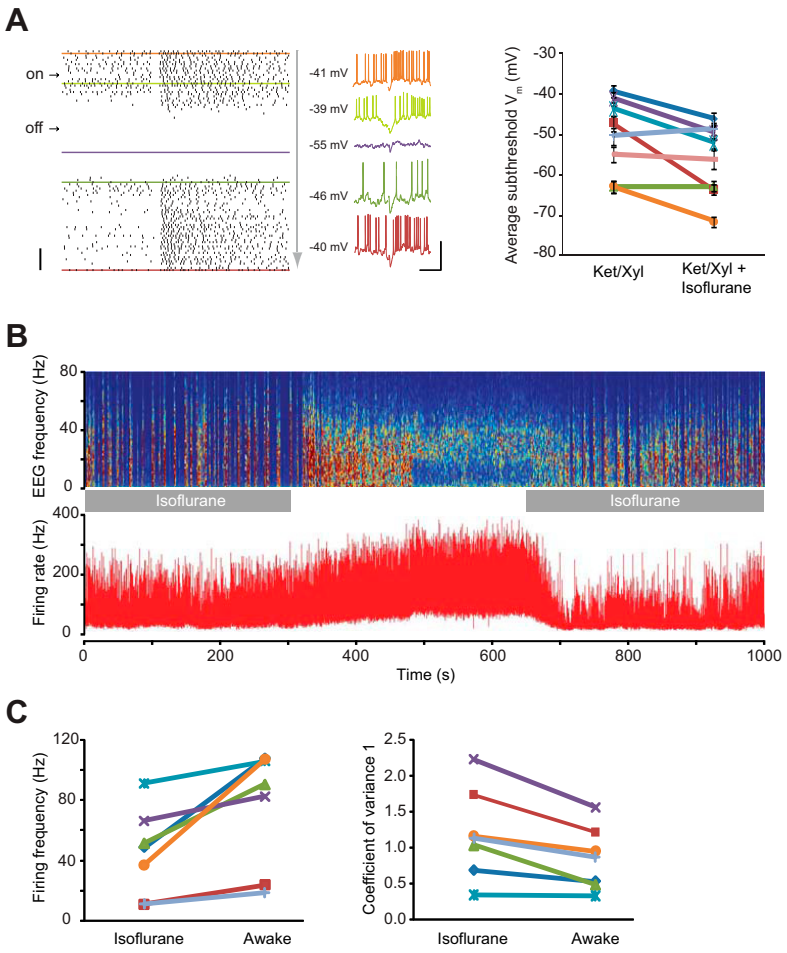

Fig. S3. The effect of isoflurane on CN activity patterns. (*A*) (*Left*) Representative raster plot of whole cell recordings in vivo of a CN neuron before (*Upper*), during (between "on" and "off"), and after (*Lower*) the coapplication of isoflurane. Vertical gray arrow indicates the time-line of the experiment, vertical scale bar indicates 20 s. Horizontal colored lines in the raster plot correspond to the colored traces next to it. [Scale bars, 50 ms (horizontal) and 20 mV (vertical).] Note that the effects of isoflurane are fully reversible. To obtain such stable recordings, mice were first anesthetized with ketamine/xylazine as normal (*SI Materials and Methods*). After a stable baseline was obtained for > 1 min, isoflurane (1.75% in O_2 and air) was coapplied (marked "on" next to the raster plot). Before the application of isoflurane, this typical CN neuron showed continuous firing and pronounced rebound activity; after coapplication of isoflurane, CN neurons tended to show a lower firing frequency and less pronounced rebound firing ($n = 8$). (*Right*) Isoflurane application hyperpolarized the membrane potential (V_m) of six out of eight CN neurons. On average, the subthreshold membrane potential decreased significantly after the coapplication of isoflurane ($n = 8$; $P = 0.025$; paired Student's t test). (*B*) (*Upper*) Surface plot of EEG activity recorded from the left motor cortex (*SI Materials and Methods*) during a consecutive isoflurane-awake-isoflurane (2.5% in O_2) sequence with the accompanying firing rate of a typical CN neuron (*Lower*). Note the temporal increase in firing rate during the wakeful state. (*C*) (*Left*) The average firing frequency of spontaneous activity in CN neurons under isoflurane was lower than in the awake state, while the coefficient of variance 1 was increased (*Right*), indicating that CN neuron activity is slower and more irregular in isoflurane-anesthetized mice.

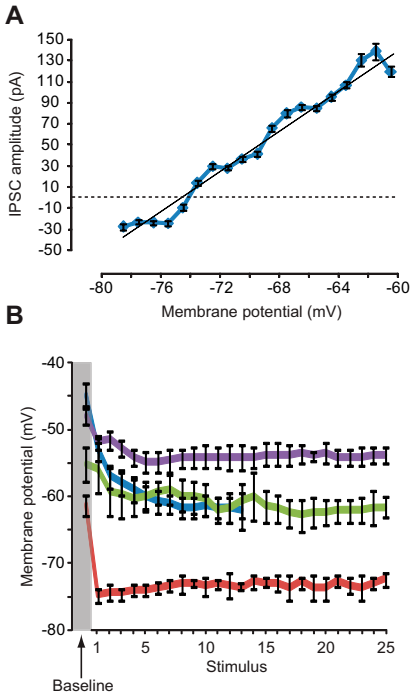

Fig. S4. (*A*) Reversal potential of cerebellar cortically evoked inhibitory events in representative CN neurons averaged over five trails. Neurons were recorded in voltage clamp mode at membrane potentials ranging from −60 to −79 mV; their responses were evoked by stimulating the cerebellar cortex with a single pulse (100 μs, 100–1,000 μA). Events reversed (dotted line) at a membrane potential of −74 mV, which is in line with the activation of $GABA_A$-receptors conducting chloride ions. (*B*) During train stimuli, the membrane potential generally did not reach the average chloride reversal potential (*A*). Indicated are recordings of four CN neurons, during which 10 subsequent trials of a train of 13 to 25 stimuli at 100 Hz were applied to the cerebellar cortex. Average subthreshold membrane potentials are indicated in the grey bar.

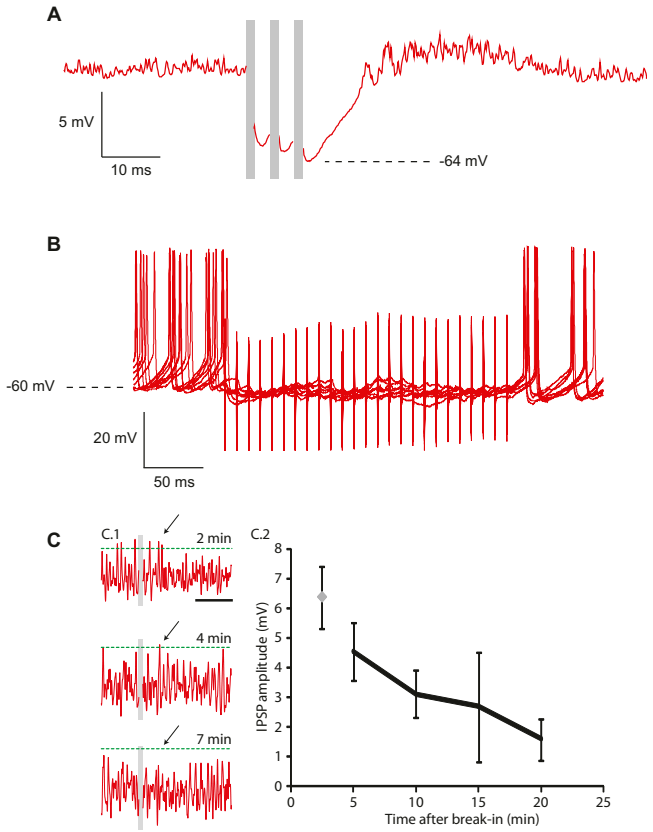

Fig. S5. (*A*) Electrical stimulation of the cerebellar cortex with three pulses at 250 Hz faithfully evokes three consecutive IPSPs in CN neurons. The red trace indicates the average of 50 such trials of a typical recording. Gray bars represent the stimulus artifact. This particular neuron hyperpolarized to −64 mV. (*B*) Stimulating at 100 Hz also faithfully evoked IPSPs in CN neurons as shown by this overlay of seven traces of a typical recording. (*C*) Responses of CN neurons to stimulation with three pulses at 250 Hz applied to the cerebellar cortex, in which inhibitory input was partially blocked. Blocking inhibitory input onto CN neurons was accomplished by substituting 5-mM sucrose for 5-mM 4,4′-Difluoro-3,3′-dinitrodiphenyl sulfone (DNDS; Sigma-Aldrich) [Dudek SM, Friedlander MJ (1996) Intracellular blockade of inhibitory synaptic responses in visual cortical layer IV neurons. *J Neurophysiol* 75:2167–2173.] in the electrode medium (see *SI Materials and Methods*). *C1*: Gaussian-convolved (Fig. 2 and Fig. S2) representation of spiking chance showed timed-spiking (arrow) following stimulus-induced IPSPs (gray bar) upon break-in (*Top*), which faded over the next 5 min (*Middle* and *Bottom*). (Scale bar, 100 ms.) *C2*: IPSP amplitudes gradually decreased over time from 6.4 ± 1.1 pA (values from CN neurons recorded without DNDS in the pipette; grey diamond) (Fig. 2*H*) to 1.6 ± 0.7 pA ($n = 5$; $P < 0.01$) at 20 min after break-in using DNDS-containing pipettes.

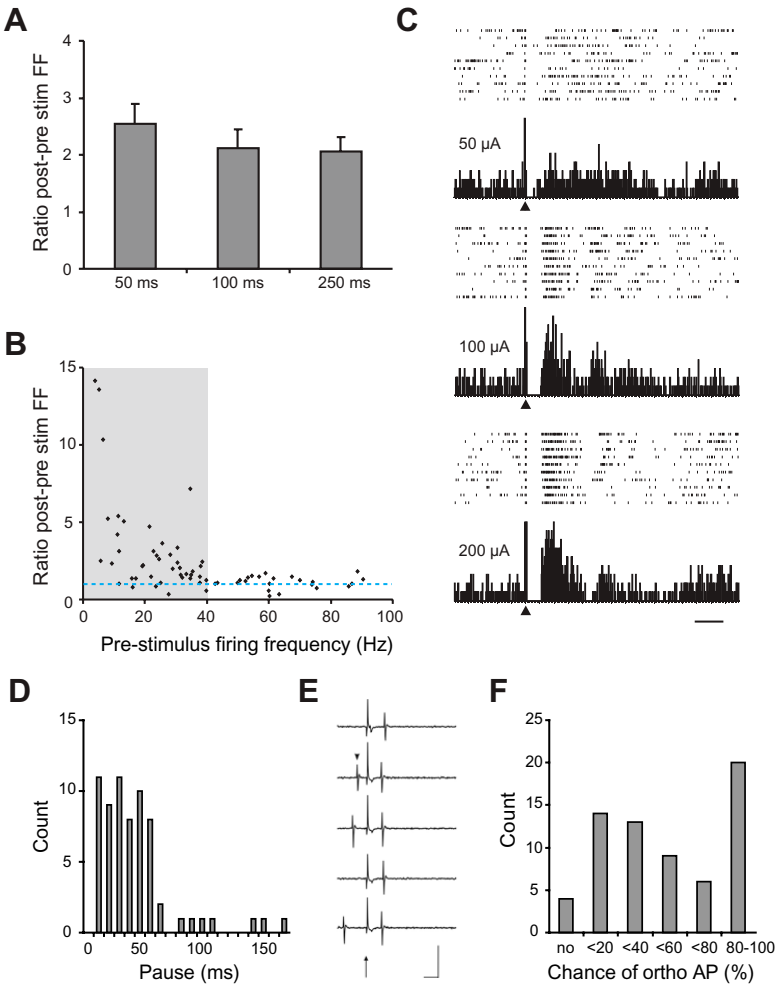

Fig. S6. *(A)* Average group ratio of mean firing frequency determined over 50, 100, or 250 ms after termination of the pause (poststimulus) and 250 ms before the stimulation (prestimulus) ($n = 66$). The average firing frequency of all three poststimulus groups was significantly higher than the prestimulus average ($P < 0.0001$, paired Student's t test). (*B*) Units that have a spontaneous firing frequency of < 40 Hz (gray box) show the highest rations of post- *re* prestimulus firing frequency. Dashed horizontal line indicates no change in firing frequency following the stimulus-induced pause. (*C*) Graded stimulation of the inferior olive (IO) results consistently first in a pause and subsequently in a rebound response. Note that evidence of a second period of increased activity can be noted, which may reflect the induction of an oscillatory rebound in the IO caused by the stimulation (main text and Fig. 3*E*). (Scale bar, 100 ms.) *(D)* Distribution of the duration (in milliseconds) of the pause determined in 66 responsive CN neurons. *(E)* Example of CN neuron firing an action potential with a consistently short latency (5.4 ± 0.1 ms) to consecutive stimulations of the IO (arrow). Note that a spontaneously occurring action potential (arrowhead) did not collide with the orthodromically triggered spike, indicating that this spike was not activated antidromically. (Scale bars, 5 ms and 0.5 mV.) *(F)* Distribution indicating reliability of orthodromically triggered spikes by IO stimulation. In 20 out of the 66 units, this spike was very consistently triggered (>80%).